

# Hyperspectral-LIDAR system and data product integration for terrestrial applications

Lawrence A. Corp<sup>1</sup>, Yen-Ben Cheng<sup>2</sup>, Elizabeth M. Middleton<sup>3</sup>, Geoffrey G. Parker<sup>4</sup>  
K. Fred Huemmrich<sup>5</sup>, Petya K. Entcheva Campbell<sup>5</sup>

<sup>1</sup>Sigma Space Corporation, Lanham, MD 20706

<sup>2</sup>Earth Resources Technology Inc., Annapolis Junction, MD 20701

<sup>3</sup>Biospheric Sciences Branch, NASA/GSFC, Greenbelt, MD 20771

<sup>4</sup>Smithsonian Environmental Research Center, Edgewater, MD 21037

<sup>5</sup>Joint Center for Earth Systems Technology, UMBC, Baltimore, MD 21250

## ABSTRACT

This manuscript details the development and validation of a unique forward thinking instrument and methodology for monitoring terrestrial carbon dynamics through synthesis of existing hyperspectral sensing and Light Detection and Ranging (LIDAR) technologies. This technology demonstration is directly applicable to linking target mission concepts identified as scientific priorities in the National Research Council (NRC, 2007) Earth Science Decadal Survey; namely, DESDynI and HypIRI. The primary components of the Hyperspec-LIDAR system are the ruggedized imaging spectrometer and a small footprint LIDAR system. The system is mounted on a heavy duty motorized pan-tilt unit programmed to support both push-broom style hyperspectral imaging and 3-D canopy LIDAR structural profiling. The integrated Hyperspec-LIDAR sensor system yields a hyperspectral data cube with up to 800 bands covering the spectral range of 400 to 1000 nm and a 3-D scanning LIDAR system accurately measuring the vertical distribution of intercepted surfaces within a range of 150 m with an accuracy of 15 mm. Preliminary field tests of the Hyperspec-LIDAR sensor system were conducted at a mature deciduous mixed forest tower site located at the Smithsonian Environmental Research Center in Edgewater, MD. The goal of this research is to produce integrated science and data products from ground observations that will support satellite-based hybrid spectral/structural profile linked through appropriate models to monitor Net Ecosystem Exchange and related parameters such as ecosystem Light Use Efficiency.

**Keywords:** Remote Sensing, Vegetation, Imaging Spectroscopy, LIDAR, Carbon Cycle Science

## 1. INTRODUCTION

Direct estimation of carbon storage in moderate to high biomass forests remains a major challenge for remote sensing<sup>[1,2]</sup>. While remote sensing has had considerable success in measuring the biophysical characteristics of vegetation in areas where plant canopy cover is relatively sparse, quantification of vegetation structure where leaf area index (LAI) exceeds three has been less successful<sup>[3,4,5]</sup>. High LAI forests, which generally have high above-ground biomass, occur in the boreal, temperate and tropical regions. These forests cover less than 35% of the Earth's terrestrial surface, yet account for 67% of terrestrial net primary productivity (NPP) and 89% of terrestrial biomass<sup>[6]</sup>. Given their prominent role in global biogeochemistry and the likelihood that these high productivity areas will be prime areas for carbon sequestration efforts, better characterization of high biomass forests using remotely sensed data is desirable.

To understand the dynamics of carbon uptake, both the light environment and canopy physiology must be considered. An integrated approach that simultaneously resolves both the spectral and structural properties of the canopies is needed to isolate sunlit portions of tree crowns and to account for changes in underlying terrain. Whereas the spectral signatures can be derived from hyperspectral imaging spectrometers<sup>[7]</sup>, the canopy structure and terrain data are often best resolved using Light Detection and Ranging (LIDAR)<sup>[1]</sup>. For forests, relating LIDAR information to conventional, primarily non-spatial, measurements of forest structure, such as above-ground biomass and stand basal area, has been a primary research goal<sup>[2,8,9]</sup>. However, the coordinated use of these two technologies, especially in the context of detailed crown-by-crown mapping of species, requires precise collocation of the spectrometer and LIDAR data<sup>[10]</sup>.

The focus of this article is to describe the development and validation of a unique forward thinking instrument and innovative methodology for monitoring terrestrial carbon dynamics through synthesis of existing hyperspectral sensing and LIDAR technologies. This technology demonstration is directly applicable to the near term missions listed in the National Research Council's Decadal Survey. In particular, successful implementation of this technology would support and link two mission concepts identified in the Decadal Survey; namely, DESDynI (first tier, 2010-2013) and HypsIRI (second tier, 2013-2016)<sup>[11]</sup>. These mission concepts focus on overlapping sets of science objectives related to the assessment of both canopy structure and physiology. In terms of satellite observations, these two measurements do not need to be made simultaneously, but could be separated by up to a few weeks because ecosystem structure typically does not change significantly on short time scales without a disturbance event. Due to the instrument-centric approach in the design of the Decadal Survey missions, efforts to fuse data from LIDAR and hyperspectral sensors are lagging. As a science community we cannot successfully understand vegetation dynamics, in terms of carbon exchange, water budget, biodiversity, or the early detection of stress responses that may be the precursors to disturbance events without understanding the interaction of structure and physiology.

Vegetation structure and physiology are fundamentally linked, with structure defining the spatial distribution of leaves that, in combination with incident Photosynthetically Active Radiation (PAR), defines the light environment the leaves experience. The light environment, in turn, is a key factor determining the physiological state of the leaves. This affects the overall rate of carbon uptake and transpiration of water, as well as the spectral reflectance of the canopy. Thus, this study combines the use of spectral information to measure vegetation physiological properties with remotely sensed structural measurements (canopy height, vertical profile, volume) to improve our understanding of ecosystem function. Integrated data sets of hyperspectral and LIDAR profiles will provide improved metrics over use of either data set alone in evaluating vegetation condition. The integrated science and data products from the proposed project will support a rigorous satellite-based hybrid spectral/structural profile linked through models to monitor net ecosystem exchange (NEE) and related parameters such as ecosystem photosynthetic light use efficiency (LUE). A method to synoptically estimate LUE from space would provide more accurate time-varying parameters for input to gross primary productivity (GPP) models and improve current global net primary productivity (NPP) products.

The fundamental goal of the Hyperspec-LIDAR system and associated research is to facilitate the development of statistically rigorous and a viable hybrid remote sensing approach to using narrow band hyperspectral observations, radiative transfer/physiological models, and measurements of the horizontal and vertical canopy structure to monitor NEE, GPP and LUE, that can be adapted for use from space-borne satellite platforms. In accomplishing this goal, an instrument system is needed to support the key technology developments and resolve challenges related to combining data products from LIDAR instruments (e.g., DESDynI) and hyperspectral imagery (e.g., HypsIRI) from future NASA satellite missions. The specific milestones of this study are as follows: (1) produce an integrated Hyperspec-LIDAR sensor system consisting of a push-broom Hyperspectral Imager combined with a 3-D LIDAR system; (2) perform field tests of the Hyperspec-LIDAR sensor system in conjunction with the supporting ground measurements over contrasting vegetation types; (3) produce integrated science and data products that will support satellite-based hybrid spectral/structural profiles to monitor NEE and related parameters such as ecosystem LUE.

## **2. INSTRUMENT SPECIFICATIONS**

### **2.1 Hyperspec Imaging Spectrometer**

The major components of the hyperspectral imaging system are comprised of the Hyperspec™ VNIR Concentric Imaging Spectrometer (Headwall Photonics, Fitchburg, MA), the ruggedized RA1000m/D digital fine gain imaging camera (Adimec, Stoneham, MA). The Hyperspec spectrometer enables high spectral and spatial resolution imaging through high efficiency f/2.0 telecentric optics and a high efficiency aberration-corrected convex holographic diffraction grating, providing an optical dispersion of 100 nm per mm over a 7.4 mm spatial by 6.0 mm spectral focal plane. The concentric spectrograph, based on the Offner design, enables imaging from 400-1000 nm over the full extent of an 18 mm tall user interchangeable entrance slit. The standard slit width used in this work was 12.5 microns wide, yielding a 1.29 nm spectral resolution. Hyperspec imaging spectrometer accepts a C-mount objective lens that is field interchangeable, providing the ability to vary the FOV and IFOV within the application scene. The Xenoplan f/1.4 17mm and f/1.9 35mm objective lenses (Schneider Optics, Hauppauge, NY) were selected to provide high optical performance using ultra low dispersion glass and special broadband anti-reflection coating designed for enhanced visible to near-IR precision imaging. Coupled to the spectrometer is the RA1000m/D high speed rugged megapixel camera

allowing the acquisition of up to 50 progressive frames per second acquired through the PIXCI ECB1 (EPIX Inc., Buffalo Grove, IL) notebook computer using a PCI ExpressCard base CameraLink interface. The camera uses a 1/2 inch interline 12 bit CCD imager in a 1004x1004 format with 7.4 micron pixels. Camera features include: a digital fine gain for adjustable camera sensitivity over a 60 dB dynamic range, electronic shuttering, low smear characteristics, and offers ruggedized military specifications for severe operating environments. The camera is fully software controlled via a ruggedized notebook computer and the serial communication channel of the CameraLink interface. Image acquisition, motion control, and hyperspectral data cube generation are accomplished through the customized Hyperspec<sup>TM</sup> acquisition software with LabVIEW executable graphic user interface.

## 2.2 Light Ranging and Detection (LIDAR)

The Riegl LD90-3100HS single point laser range finder operating at 200 Hz was operated with the hyperspectral imager. This portion of the system accurately measures the distance between the canopy top (minimum distance function) and ground elevation (maximum distance function) along with the average vertical distribution of intercepted surfaces within a range of 150 m with an accuracy of  $\pm 15$  mm. The class 1 laser diode emits at 930 nm with a beam divergence of 1.8 mrad after collimating optics to yield a 0.18 cm beam diameter per meter of distance. The LIDAR data yields a basic geometric representation of vegetation topography where structure can be resolved with reasonable accuracy<sup>[12]</sup>.

## 2.3 Pan-Tilt Motion Control

The Hyperspec-LIDAR system was mounted on an optical breadboard measuring 30 x 50 cm and attached to a heavy duty programmable pan-tilt unit (DP300, Directed Perception, Burlingame, CA), with a combined sensor payload of 15 lb (Fig. 1). The DP300 pan tilt unit enables push broom hyperspectral data collection with a user selected pan increment up to 360° continuous and tilt view zenith from 0° to 120°. Both pan and tilt axis have an adjustable speed up to 22° per second with 0.00625° position accuracy. The motorized pan-tilt unit was custom programmed to enable push-broom style hyperspectral imaging along with 3-D canopy structure profiling. The system mount provides computer controlled motorized pan and tilt positioning to enable hyperspectral reflectance survey (pan sweep) and bi-directional reflectance profiling (tilt sweep) from a stationary observation platform. In addition, considerable amount of effort has been placed on this system design and interoperability of individual components, mechanical integration, and defining software requirements.

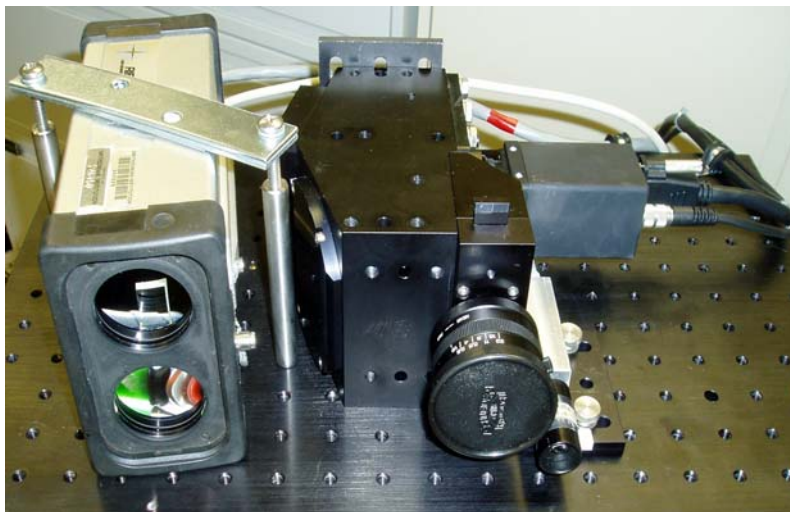


Fig. 1. The Hyperspec-LIDAR is comprised of an optical sensor head containing the Riegl LD-90 laser range finder, a hyperspectral imager (400 to 1000 nm at 0.75 nm increments), and an upward looking spectrometer to accurately measure irradiance.

### 3. DATA ACQUISITIONS

#### 3.1 Laboratory Operation

Hyperspectral imagery of the tropical cane plant (*Dieffenbachia bowmannii*, Araceae) was obtained in the laboratory under four 500W tungsten lamps. The hyperspectral-LIDAR acquisition covered a field of view of 1.5m H x 0.75m W with an average range of 1 m to the target. The plant was selected for its large variegated leaves and complex structure. A true color (RGB: 650, 550, 480 nm) composite image of the plant is displayed in the left most panel of Figure 2. Three commonly used vegetation indices spanning the VIS-NIR spectral range of the sensor are displayed in three middle panels of figure 2 with a rainbow false color applied such that blue hues indicate low index values ranging to red which indicate high index values. The  $ND_{705}$  index calculated as the normalized difference of two wavebands in the red-edge region of the spectrum  $[(R_{750}-R_{705}) / (R_{750}+R_{705})]$  is a hyperspectral modification of the more traditional broadband normalized difference vegetation index (NDVI) and is most commonly used for vegetation stress detection<sup>[13,14]</sup>. Here the index clearly depicts the variegated leaf attributes with dark hues and identifies more productive regions of the plant containing higher concentrations of photosynthetic pigments with light hues. The Photochemical Reflectance Index  $[PRI = (R_{531}-R_{570}) / (R_{531}+R_{570})]$  is a reflectance measurement that is sensitive to changes in carotenoid pigments (particularly xanthophyll pigments) in live foliage. Carotenoid pigments are indicative of photosynthetic light use efficiency, or the rate of carbon dioxide uptake by foliage per unit energy absorbed and is used in studies of vegetation productivity and stress<sup>[15]</sup>. PRI operated inverse to the  $ND_{705}$  index with light hues indicating high carotenoid contents and low productivity (Fig. 2, center). The Water Band Index ( $WBI = R_{900}/R_{970}$ ) is a reflectance measurement that is sensitive to changes in canopy water status. As the water content of vegetation canopies increases, the strength of the absorption around 970 nm increases relative to that of 900 nm and applications include canopy stress analysis<sup>[16]</sup>. Here the WBI index indicates the spatial distribution of water throughout the plant with light hues indicating higher water contents. The 3-D co-registered LIDAR composite image is shown in the left most panel of Figure 2 with dark hues indicating plant components close to the sensor ranging to light hues for components farther from the sensor. The LIDAR system tests indicate that the single point return system operating on a motorized pan tilt provides adequate scanning performance to resolve plant structural attributes.

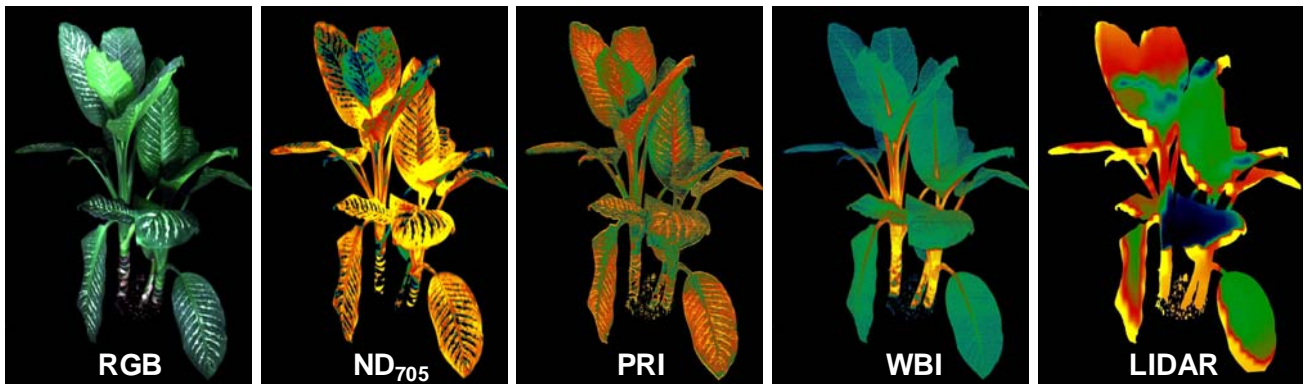


Fig. 2. Laboratory operation of the Hyperspec-LIDAR instrument on a tropical cane plant, with true color band selection on the left, three commonly used vegetation indices displayed in the middle, and the LIDAR plant profile on the right. The high resolution spatial/spectral information can be used to track plant biochemical and structural attributes.

The hyperspectral imager provides high resolution spatial/spectral information (Fig. 3) that can be applied to track biochemical attributes of the plant. Each red square in the RGB composite to the left represents a 100 pixel window from which the average spectra from the 800 band image is shown to the right. Here reflectance was obtained by dividing the DN pixel values by a reference illumination and applying a flat field correction. The 0.75 nm spectral sampling interval provides clear spectral attributes associated with distribution of plant pigments within the variegated leaves. The sharp rise in the red-edge region from 650 to 750 nm is primarily driven by chlorophyll with a blue shift under low chlorophyll conditions (Fig 3, top left). Also under limiting chlorophyll, plant carotenes have a greater impact increasing visible spectral reflectance from 450 to 600 nm. NIR reflectance from 750 to 1000 nm is primarily driven by leaf structure and water content which for this sample is fairly constant across the leaf surface.

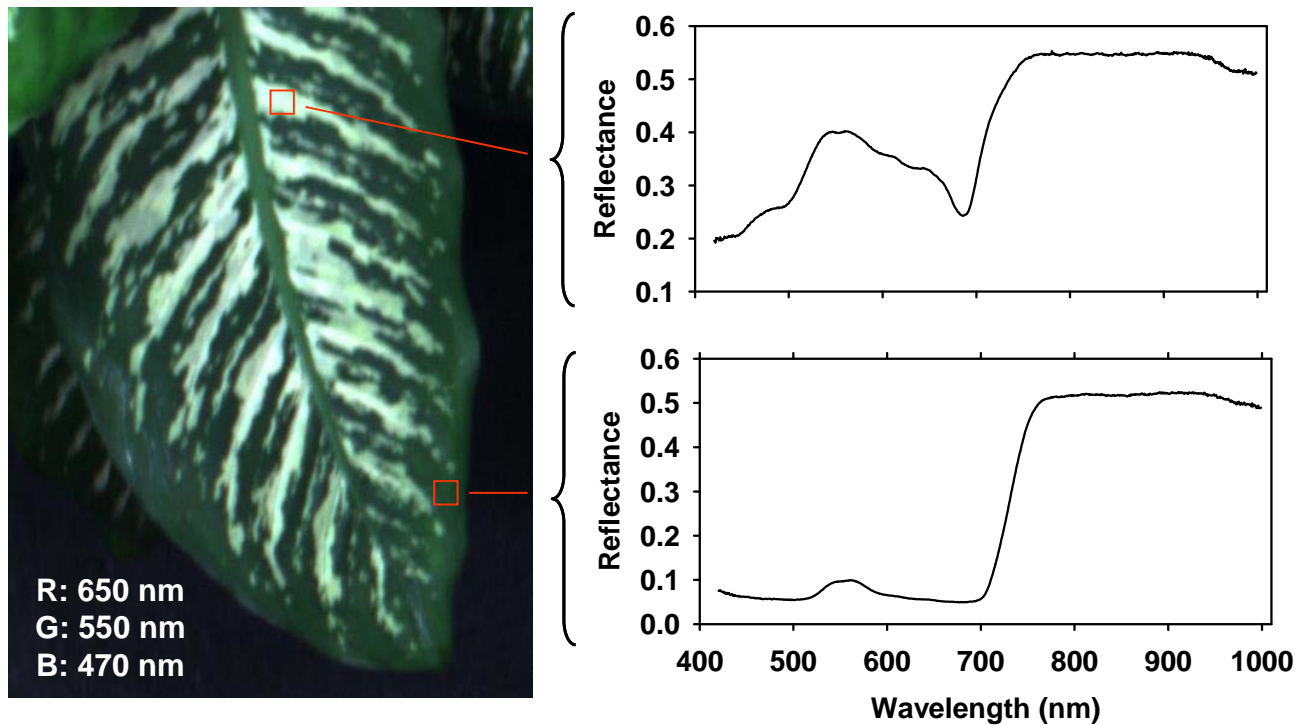


Fig. 3. Zoom in on leaf from figure 2 with true color band selection on the left and spectra (Z-profile) corresponding to variegated (top) and high chlorophyll containing green leaf portions (bottom). The impact of chlorophyll light absorption is clearly evident in the reflectance spectral region from 400 to 750 nm while leaf structure and water content are relatively unchanged from 750 to 1000 nm.

### 3.2 Smithsonian Environmental Research Center (SERC) Tower Operation

The SERC site is located in Edgewater, MD and contains an extensive hardwood forest tract of 2 km continuous mature poplar dominated mixed forest with a maximum height of about 40 meters. The leaf-area density distribution has understory and overstory peaks, which makes this site an excellent case study. The SERC forest has been well characterized with regular measurements of diameter at breast height (DBH), light transmission, and litterfall. An instrumented tower is located at 38°53'24"N by 76°33'36"W in a contiguous section of the poplar dominated mixed forest. The hyperspectral-LIDAR sensor was installed on a 50 m instrumented tower in May-July 2009 and acquired data pointing off-NAIR at a minimum range of 15 m to the forest canopy.

#### 3.2.1 Hyperspectral Acquisitions

For tower operation calibration images of a 50% spectralon reference are collected at the start and end of each acquisition sequence. These readings are used for irradiance and flat field optical corrections. A sample hyperspectral data acquisition is shown in Figure 4 with the solid shaded box indicating the image acquisition area with the diurnal sun track indicated as dashed orange lines becoming solid during the acquisition period. Local solar time and cardinal coordinates are marked along the outer circumference. Metadata for each image acquisition are also stored in a table format indicating the start and end points for; cardinal position, local time, solar azimuth, solar zenith, relative sensor pan and tilt coordinates. This information is then used to obtain co-registered LIDAR data cutouts of matching dimension.

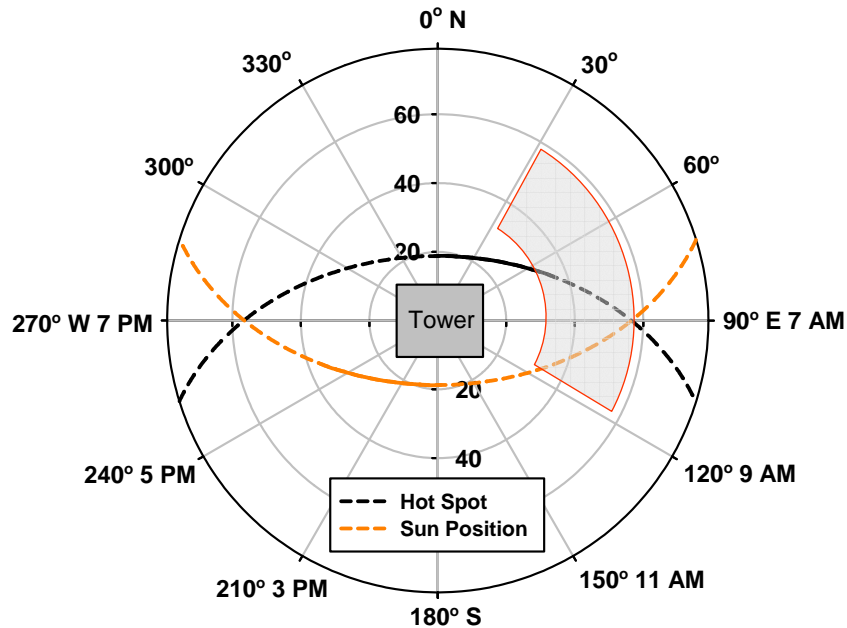


Fig 4. Polar plots indicating sun position and reflectance hot spot coordinates and image acquisition area (shaded). Major cardinal directions are marked along the outer circumference with the angular theta coordinates for solar/view azimuth while zenith angles are plotted on the radial axis. Solar positions were calculated for the image acquisition date of May 21,2009 for the mid-Atlantic SERC tower coordinates of 39° 01' N by 76° 50' W.

### 3.2.2 LIDAR Acquisitions

Once forest canopies reach full leaf-out the hyperspectral and LIDAR measurements do not need to be made simultaneously and could be separated by up to a few weeks since ecosystem structure typically does not change significantly on short time scales without a major disturbance event. As a result, one complete 360° LIDAR sweep from near NADIR to the horizon would supply canopy structural attributes for several hyperspectral acquisitions. The RIEGL LD90 operating at 200 Hz was set to transmit the average return of a 20 shot integration period. The pan speed of the DP300 unit was set such that the horizontal frequency of LIDAR observations would match the scanning pixel dimension of the Hyperspec imager. The vertical tilt axis was programmed to collect in 1° increments and data points were interpolated such that the final dimension of the LIDAR product matched the 1004 vertical spatial pixels of the Hyperspec imager. The LIDAR data was then displayed as an image, common ground control points were visually selected, and LIDAR image was warped to co-register with the hyperspectral data cube.

### 3.2.3 Hyperspec-LIDAR combined data products

A co-registered segment of the Hyperspec-LIDAR acquisition is shown in Figure 5. In the top left is a true color image with three regions of interest. Region (A) is a far field oak dominated sunlit crown with a mean range of 28 m from the instrument. The second region (B) is dominated by shaded understory with a wide range of LIDAR returns from 26 to 35 m. The third region (C) is a near field poplar dominated sunlit upper crown with a mean range of 20 m. The square defining each region is 100 X 100 pixels yielding 10,000 pairs of spectra and LIDAR data points. Mean spectra for each region are plotted in Figure 5 (top right). The sunlit upper oak and poplar upper tree crown has similar spectral features with the oak having a higher NIR reflectance than poplar. The converse is observed in the green and yellow region from 500 to 675 nm which is most likely attributed to the poplar blossoms. The shaded understory region (C) has a dramatically reduced signal with the NIR region yielding only 20% reflectance.

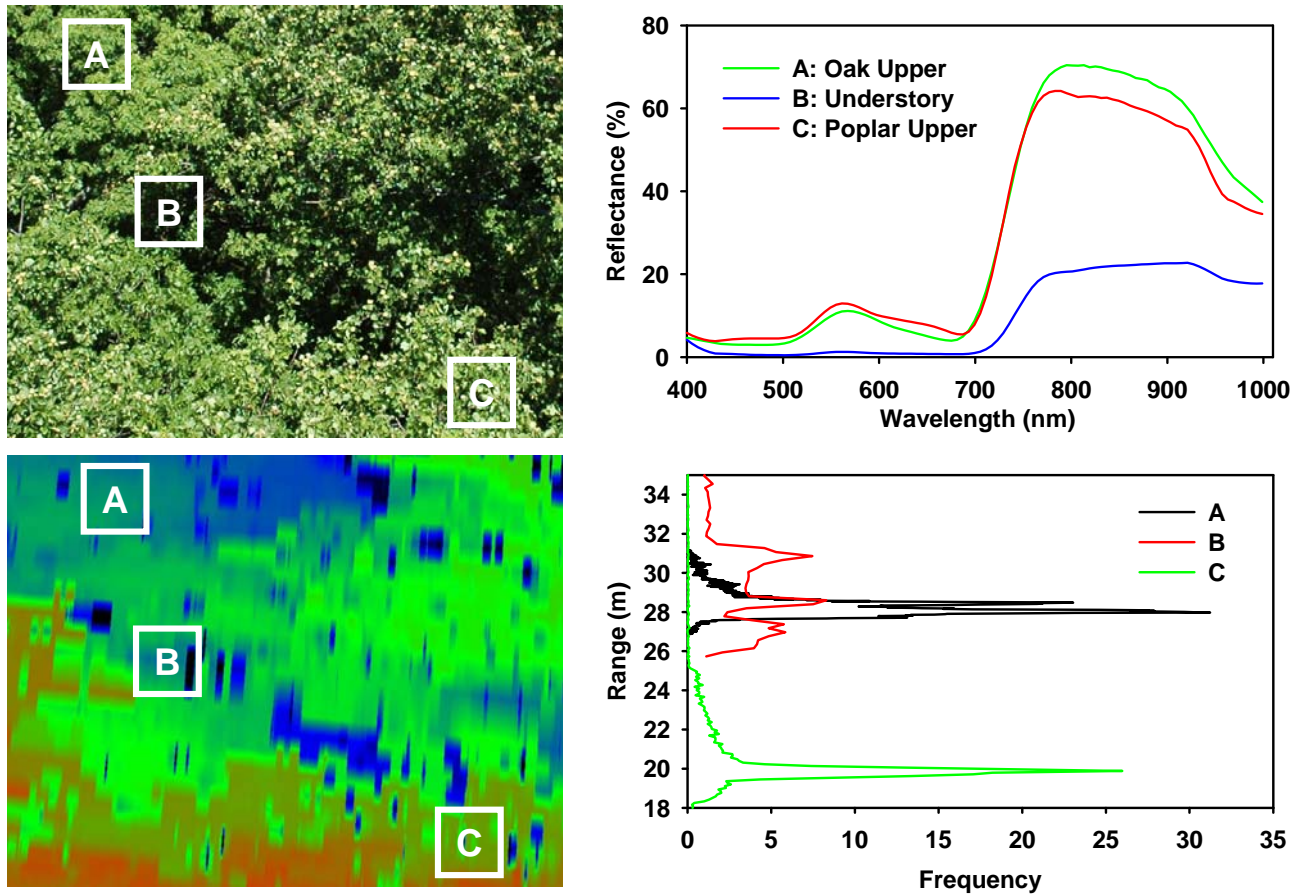


Fig. 5. Hyperspec-LIDAR data acquisition from SERC tower. True color image (top left) and LIDAR false color composite (bottom left) with three varying canopy regions of interest labeled A through C. Reflectance spectra averaged from each region of interest (10K pixels) are shown in upper left along with frequency distributions for LIDAR average returns (bottom left).

LIDAR returns are shown graphically in Figure 5 (bottom left). A rainbow color scale was applied with the shortest laser returns depicted in red and the farther returns in black. Canopy gaps with shaded understory are readily apparent with sudden transitions from light to dark hues. The three tree crowns which dominate this scene can be identified with; the cluster of red pixels defining a near-field poplar crown, green pixels defining the mid-range poplar crown, and the blue-green pixels defining a far-field oak crown. The frequency distribution of LIDAR returns corresponding to each region of interest are displayed in Figure 5 (bottom right). For regions A and C, the distributions are narrow indicating a relatively homogeneous sampling of the respective upper-story sunlit oak and poplar crowns. In contrast, region B has multiple peaks associated with a complex sampling of forest scene. Imaging spectroscopy alone does offer visual clues as to the complexity of regions being sampled but the added LIDAR information can provide a statistically rigorous basis for establishing canopy architecture. Spectral algorithms can potentially be applied to this scene mapping areas of high and low photosynthetic productivity but this information would only apply to the surface view of this complex canopy. The LIDAR data allow us to predict canopy volume leading to more accurate estimates of GPP.

## 4. DISCUSSION

LUE of forests exhibits significant temporal and spatial dynamics<sup>[17,18]</sup>, with variations throughout forest canopies dependent on illumination status, with clear differences for foliage in direct sunlight versus in shadow or diffuse PAR. LUE is strongly affected by the ratio of diffuse to direct PAR, a parameter that summarizes the effects of sun angle and atmospheric conditions on the incoming PAR, describing the available canopy light environment. This partitioning of light in the canopy, resulting in different physiological states for sunlit and shaded foliage fractions, is captured in the directional dynamics of spectral indices such as the Photochemical Reflectance Index (PRI). The PRI utilizes 531 nm as an indicator of high light stress, relative to a defined reference band. The sunlit foliage subset dominates the hotspot backscatter signal in remotely acquired directional spectral reflectance. The shaded canopy fraction is correlated with total leaf area index (LAI) in closed canopy forests, and defines the coldspot (forward) volume scatter signal for spectral reflectance. Under cloudy skies, this partitioning is minimized or lacking, so that the LUE of upper (most exposed) foliage is similar to that of foliage in the lower canopy.

Investigators from the University of British Columbia, an Automated Multi-angular Spectralradiometer (AMspec) composed of a radiometer on a motor driven probe was successfully used to measure year round spectral reflectance under different view and sun angles from a Fluxnet-Canada eddy covariance flux tower monitoring a Douglas-fir dominated forest site<sup>[19]</sup>. Spectral investigations such as this are limited in scope due to the inability to spatially differentiate information within the sensors instantaneous field of view. The hyperspectral image data cube from the Hyperspec-LIDAR sensor system provides a unique sensing capability to interactively analyze individual components within the vegetative scene and strengthen the data quality and capabilities well beyond those of the AMspec observations. To plan for future hyperspectral satellites, new studies are critical to define the optimal narrow band information required for monitoring ecosystem health from space. High spectral resolution reflectance data obtained for vegetation over a range of functional types, species, phenology, and stress conditions will be evaluated to establish which spectral algorithms perform rigorously with respect to correlation to photosynthetic function and efficiency. Further research is needed to better define and demonstrate the synergistic use of imaging spectroscopy and LIDAR canopy profiles.

## 5. CONCLUSIONS

This effort identified a viable hybrid remote sensing approach for using narrow band hyperspectral observations and measurements of the horizontal and vertical canopy structure with strong implications to monitor GPP and LUE. An integrated Hyperspec-LIDAR sensor system consisting of a push-broom Hyperspectral Imager combined with a 3-D LIDAR system was assembled and tested on a tower over a mixed deciduous forest. The Hyperspec concentric imaging spectrograph provided hyperspectral imaging with 800 bands evenly spaced at 0.75 nm over the spectral range of 400-1000 nm at 1.29 nm FWHM spectral resolution. The Riegl LD90-3100HS single point laser range finder accurately measured the average vertical distribution of intercepted surfaces within a range of 150 m with an accuracy of  $\pm 15$  mm. The integrated science and data products from this system have the potential to support satellite-based hybrid spectral/structural profiles to monitor NEE and related parameters such as ecosystem LUE.

## REFERENCES

- [1] Lefsky, M. A., Cohen, W. B., Harding, D. J., Parker, G. G., Acker, S. A. and Gower, S. T., "Lidar remote sensing of aboveground biomass in three biomes," *Global Ecology and Biogeography* 11:393-400 (2002).
- [2] Lefsky, M. A., Cohen, W. B., Parker, G. G. and Harding, D. J., "Lidar remote sensing for ecosystem studies," *BioScience* 52:19-30 (2002).
- [3] Waring, R.H., Way, J., Hunt, E.R., Morrissey, L., Ranson, K.J., Weishampel, J.F., Oren, R. and Franklin, S.E., "Imaging radar for ecosystem studies," *Bioscience*, 45, 715-723 (1995).
- [4] Carlson, T.N. and Ripley, D.A., "On the relation between NDVI, fractional vegetation cover, and leaf area index," *Remote Sensing of Environment*, 62, 241-252 (1997).
- [5] Turner, D., Cohen, W., Kennedy, R., Fassnacht, K. and Briggs, J., "Relationship between leaf area index and Landsat TM spectral vegetation indices across three temperate zone sites," *Remote Sensing of Environment*, 70, 52-68 (1999).

- [6] Waring, R.H. and Schlesinger, W.H., "Forest ecosystems: concepts and management," Academic Press, Orlando, Florida (1985).
- [7] Clark, M. L., Roberts, D. A. and Clark, D. B., "Hyperspectral discrimination of tropical rain forest tree species at leaf to crown scales," *Remote Sensing of Environment*, 96, 375–398 (2005).
- [8] Means, J.E., Acker, S.A., Harding, D.J., Blair, B.J., Lefsky, M.A., Cohen, W.B., Harmon, M. and McKee, W.A., "Use of large-footprint scanning airborne lidar to estimate forest stand characteristics in the western Cascades of Oregon," *Remote Sensing of Environment*, 67, 298–308 (1999).
- [9] Drake, J., Dubayah, R., Clark, D., Knox, R., Blair, J., Hofton, M., Chazdon, R., Weishample, J. and Prince, S., "Estimation of tropical forest structural characteristics using large-footprint lidar," *Remote Sensing of Environment*, 79, 305–319 (2002).
- [10] Asner, G.P., Knapp, D.E., Kennedy-Bowdoin, T., Jones MO, Martin, R.E., Boardman, J. and Hughes R.F., "Invasive species detection in Hawaiian rainforests using airborne imaging spectroscopy and LiDAR," *Remote Sensing of Environment*, 112, 1942–1955 (2008).
- [11] Space Studies Board of the National Research Council, "Earth Science and Applications from Space: National Imperatives for the Next Decade and Beyond," (pp. 113-115). Washington D.C., The National Academies Press (2007).
- [12] Parker, G.G., Harding, D.J., and M.L. Berger, "A portable laser altimeter for rapid determination of forest canopy structure," *Journal of Applied Ecology* 41:755-767 (2004).
- [13] Gitelson, A.A., and Merzlyak, M.N., "Spectral Reflectance Changes Associated with Autumn Senescence of *Aesculus Hippocastanum* L. and *Acer Platanoides* L. Leaves. Spectral Features and Relation to Chlorophyll Estimation," *Journal of Plant Physiology* 143:286-292 (1994).
- [14] Sims, D.A. and Gamon, J.A., "Relationships Between Leaf Pigment Content and Spectral Reflectance Across a Wide Range of Species, Leaf Structures and Developmental Stages," *Remote Sensing of Environment* 81:337-354 (2002).
- [15] Gamon, J.A., J. Penuelas, and Field, C.B., "A Narrow-Waveband Spectral Index That Tracks Diurnal Changes in Photosynthetic Efficiency," *Remote Sensing of Environment* 41:35-44 (1992).
- [16] Penuelas, J., I. Filella, C. Biel, L. Serrano, and R. Save, 1995. The Reflectance at the 950-970 Region as an Indicator of Plant Water Status. *International Journal of Remote Sensing* 14:1887-1905.
- [17] Middleton, E.M., Cheng, Y.B., Hilker, T., Black, T.A., Krishnan, P., Coops, N.C., and Huemmrich, K.F., "Linking Foliage Spectral Responses to Canopy Level Ecosystem Photosynthetic Light Use Efficiency at a Douglas-fir Forest in Canada," *Canadian J. Rem. Sens.*, in press, (2009).
- [18] Drolet, G.G., Middleton, E.M., Huemmrich, K.F., Hall, F.G., Margolis, H.A., Amiro, R., Barr, A., and Black, T.A., "Regional mapping of gross light-use efficiency using MODIS Spectral Indices," *Remote Sensing of Environment* 12: 3064-3078 (2007).
- [19] Hilker, T., Coops, N.C., Nestic, Z., Wulder, M.A., and Black, T.A., "Instrumentation and Approach for Unattended Year Round Tower Based Measurements of Spectral Reflectance," *Computers and Electronics in Agriculture* 56, 72-84 (2007).